

Ligand-Promoted Solvent-Dependent Ionization and Conformational Equilibria of $\text{Re}(\text{CO})_3\text{Br}[\text{CH}_2(\text{S-tim})_2]$ ($\text{tim} = 1\text{-methylthioimidazolyl}$). Crystal Structures of $\text{Re}(\text{CO})_3\text{Br}[\text{CH}_2(\text{S-tim})_2]$ and $\{\text{Re}(\text{CO})_3(\text{CH}_3\text{CN})[\text{CH}_2(\text{S-tim})_2]\}(\text{PF}_6)$

Rosalice M. Silva,[†] Brendan J. Liddle,[†] Sergey J. Lindeman,[†] Mark D. Smith,[‡] and James R. Gardinier^{*†}

Department of Chemistry, Marquette University, Milwaukee, Wisconsin 53213-1881, and Department of Chemistry and Biochemistry, University of South Carolina, Columbia, South Carolina 29208

Received May 5, 2006

The compounds $\text{Re}(\text{CO})_3\text{Br}[\text{CH}_2(\text{S-tim})_2]$ (**1**) and $\{\text{Re}(\text{CO})_3(\text{CH}_3\text{CN})[\text{CH}_2(\text{S-tim})_2]\}(\text{PF}_6)$ (**2**), where tim is 1-methylthioimidazolyl, were prepared in high yields and characterized both in the solid state and in solution. The solid-state structures show that the ligand acts in a chelating binding mode where the eight-member chelate ring adopts twist-boat conformations in both compounds. A comparison of both solid-state IR data for CO stretching frequencies and the solution-phase voltammetric measurements for the $\text{Re}^{1+/2+}$ couples between **1**, **2**, and related N,N -chelates of the rhenium tricarbonyl moiety indicate that the $\text{CH}_2(\text{S-tim})_2$ ligand is a stronger donor than even the ubiquitous dipyriddy ligands. A combination of NMR spectroscopic studies and voltammetric studies revealed that compound **1** undergoes spontaneous ionization to form $\{\text{Re}(\text{CO})_3(\text{CH}_3\text{CN})[\text{CH}_2(\text{S-tim})_2]^+\}(\text{Br}^-)$ in acetonitrile. Ionization does not occur in solvents such as CH_2Cl_2 or acetone that are less polar and Lewis basic (less coordinating). The equilibrium constant at 293 K for the ionization of **1** in CH_3CN is 4.3×10^{-3} . The eight-member chelate rings in each **1** and **2** were found to be conformationally flexible in all solvents, and boat-chair conformers could be identified. Variable-temperature NMR spectroscopic studies were used to elucidate the various kinetic and thermodynamic parameters associated with the energetically accessible twist-boat to twist-boat and twist-boat to boat-chair interconversions.

Introduction

There is a great deal of interest in the coordination chemistry of the tricarbonylrhenium(I) moiety because of its applications in both materials¹ and biomedical² research. One of the attractive features of tricarbonylrhenium complexes

in such applications is the generally inert nature of the metal–ligand bonds that usually gives rise to reliable, simple synthetic protocols and straightforward characterizations. We recently reported³ on the synthesis and electrochemical properties of $\text{CH}_2(\text{S-tim})_2$ ($\text{tim} = 1\text{-methylthioimidazolyl}$), a compound that contains electroactive, heterocyclic thioimidazoline ring systems but for which little is known about its coordination chemistry.^{4,5} The free ligand exhibits two one-electron oxidations (as determined by a combination of voltammetry and redox titrations), but the voltammograms

* To whom correspondence should be addressed. E-mail: james.gardinier@marquette.edu.

[†] Marquette University.

[‡] University of South Carolina.

- (1) For example, see: (a) Lewis, J. D.; Perutz, R. N.; Moore, J. N. *J. Phys. Chem. A* **2004**, *108*, 9037. (b) Pope, S. J. A.; Coe, B. J.; Faulkner, S. *Chem. Commun.* **2004**, 1550. (c) Lam, L. S. M.; Chan, W. K. *ChemPhysChem* **2001**, *2*, 252. (d) Bignozzi, C. A.; Argazzi, R.; Indelli, M. T.; Scandola, F.; Schoonover, J. R.; Meyer, G. J. *Proc. Ind. Acad. Sci., Chem. Sci.* **1997**, *109*, 397.
- (2) (a) Alberto, R.; Schibli, R.; Waibel, R.; Schubiger, A. P. *Coord. Chem. Rev.* **1999**, *190–192*, 901. (b) Volkert, W. A.; Hoffman, T. J. *Chem. Rev.* **1999**, *9*, 2269.

(3) Silva, R. M.; Smith, M. D.; Gardinier, J. R. *J. Org. Chem.* **2005**, *70*, 8755.

(4) Casas, J. S.; Castiñeiras, A.; García Martínez, E.; Rodríguez Rodríguez, P.; Russo, U.; Sánchez, A.; Sánchez González, A.; Sordo, J. *Appl. Organomet. Chem.* **1999**, *13*, 69.

(5) Silva, R. M.; Smith, M. D.; Gardinier, J. R. *Inorg. Chem.* **2006**, *45*, 2132.

were reminiscent of ECE-type behavior and, unfortunately, the nature of the oxidized products remains unclear. We therefore embarked on studies in the coordination chemistry of this ligand with the intention of finding systems that will allow for the unequivocal elucidation of the unusual electrochemical behavior of the ligand. The tricarbonylrhenium(I) complex appeared well-suited for such a study because of its anticipated inert nature and the metal's well-known electrochemical behavior. However, during the course of this study we discovered that the rhenium complexes of this ligand displayed unexpected reactivity that may prove useful to others in the future design of ligands for the tricarbonylrhenium moiety.

Experimental Section

Solvents were dried and distilled prior to use except where indicated. The syntheses of the rhenium complexes were carried out under an argon atmosphere using standard Schlenk techniques. Literature procedures were used to prepare $\text{Re}(\text{CO})_5\text{Br}$,⁶ $\text{Re}(\text{CO})_3\text{-Br}(\text{X}_2\text{-bpy})$ ($\text{X} = \text{H}, \text{Me}$),⁷ $\text{CH}_2(\text{S-tim})_2$,³ and $\{\text{Ag}_2[\text{CH}_2(\text{S-tim})_2]_2\}(\text{PF}_6)_2$.⁵ Elemental analysis was performed by Midwest Microlab Inc., Indianapolis, IN. Melting point determinations were made on samples contained in glass capillaries using an Electrothermal 9100 apparatus and are uncorrected. Infrared spectra were recorded on a Nicolet Magna-IR 560 spectrometer. ^1H and ^{13}C NMR spectra were recorded on a Varian 300 MHz spectrometer. Chemical shifts were referenced to solvent resonances at $\delta_{\text{H}} = 1.94$ and $\delta_{\text{C}} = 118.9$ for CD_3CN . Absorption measurements were recorded on an Agilent 8453 spectrometer. Electrochemical measurements were collected with a BAS CV-50V instrument for ca. 0.2 mM CH_3CN solutions of the complexes, with 0.25 M NBu_4PF_6 as the supporting electrolyte, in a three-electrode cell composed of a Ag/AgCl electrode, a platinum working electrode, and a glassy carbon counter electrode. Mass spectrometric measurements recorded in ESI(+) mode were obtained on a Micromass Q-ToF spectrometer.

$\text{Re}(\text{CO})_3\text{Br}[\text{CH}_2(\text{S-tim})_2]$ (1). A mixture of 0.340 g (0.836 mmol) of $\text{Re}(\text{CO})_5\text{Br}$ and 0.201 g (1.30 mmol) of $\text{CH}_2(\text{S-tim})_2$ in 20 mL of toluene was heated at reflux 12 h. After the mixture was cooled to room temperature, the precipitate was collected by filtration washed with two 5 mL portions of Et_2O and vacuum dried to give 0.435 g (99% yield) of analytically pure **1** as a colorless powder. mp: 233 °C (dec) gray-brown solid. Anal. Calcd (obsd): C, 24.41 (24.48); H, 2.05 (1.93); N, 9.49 (9.26). IR (CH_3CN , ν_{CO} , cm^{-1}): 2018(s), 1902, 1887. IR (KBr, ν_{CO} , cm^{-1}): 2016, 1902, 1871. ^1H NMR (CD_3CN , 293 K): δ_{H} [twist boat, 86% of signals, the following integrations are relative for only this species, see Figure 4 for labeling] 7.72 (br s, 1H, tim- H_a), 7.66 (br s, 1H, tim- H_a), 7.39 (br s, 1H, tim- H_b), 7.37 (br s, 1H, tim- H_b), 3.88 (AB multiplet, $J_{\text{AB}} = 13.2$ Hz, $\Delta\nu = 6.0$ Hz, 2H, CH_2), 3.81 (br, s, 6H, NCH_3); [boat-chair, 6% of signal, (the following integrations are relative to this species, see Figure 4 for labeling)] 8.48 (d, $J = 1.6$ Hz, 2H, tim- H_a), 7.11 (d, $J = 1.6$ Hz, 2H, tim- H_b), 4.29 (AB multiplet, $J_{\text{AB}} = 14.8$ Hz, $\Delta\nu = 47.8$ Hz, 2H, CH_2), 3.70 (br, s, 6H, NCH_3); [cation, 8% of signals, see **2**, below, for assignments] 7.58, 7.50, 7.48 (d, $J = 1.7$ Hz), 7.46, 7.25 (d, $J = 1.7$ Hz), 3.89, 3.83, 3.72; signals for one tim- H_a (twist-boat) and onset of methylene hydrogens (AB, multiplet, boat-chair) not observed

(either in baseline or overlapping more intense resonances). ESI(+) MS: 552 (13) [$\text{M} - \text{Br} + \text{CH}_3\text{CN}$], 511 (100) [$\text{M} - \text{Br}$], 411 (21) [$\text{Re}(\text{CO})_3(\text{CH}_3\text{CN})_3(\text{H}_2\text{O})^+$], 388 (18) [$\text{Re}(\text{CO})_3(\text{CH}_3\text{CN})_2(\text{H}_2\text{O})_2^+$], 370 (3) [$\text{Re}(\text{CO})_3(\text{CH}_3\text{CN})_2(\text{H}_2\text{O})^+$], 329 (50) [$\text{Re}(\text{CO})_3\text{-}(\text{CH}_3\text{CN})(\text{H}_2\text{O})^+$], 270 (7) [$\text{Re}(\text{CO})_3^+$]. HRMS Calcd (obsd) for $\text{C}_{12}\text{H}_{12}\text{N}_4\text{O}_3\text{ReS}_2$ [$\text{M} - \text{Br}$]: 510.9908 (510.9913). Single crystals suitable for X-ray diffraction were grown by slow evaporation of an acetone solution.

$\{\text{Re}(\text{CO})_3(\text{CH}_3\text{CN})[\text{CH}_2(\text{S-tim})_2]\}(\text{PF}_6)$ (2). **Method A.** A mixture of 0.105 g of ReCO_5Br (0.259 mmol) and 0.127 g (0.259 mmol) of $\{\text{Ag}_2[\text{CH}_2(\text{S-tim})_2]_2\}(\text{PF}_6)_2$ in 20 mL of CH_3CN was heated at reflux for 4 h; then, the solution was filtered through Celite, and the solvent was removed to leave crude **2** as a glassy solid. After it was washed with two 10 mL portions of Et_2O and vacuum dried, the resulting material was recrystallized by layering Et_2O onto concentrated acetonitrile solutions and allowing the solvents to slowly diffuse over 2 days. The mother liquor was decanted and the residue was vacuum dried to produce 0.170 g (94%) of analytically pure **2** as colorless plates. **Method B.** A mixture of 0.236 g (0.400 mmol) of **1** and 0.101 g (0.400 mmol) of AgPF_6 in 15 mL of CH_3CN was heated at reflux for 12 h. After the mixture was filtered and the solvent was removed by vacuum distillation, the residue was washed with two 5 mL portions of Et_2O and dried under vacuum to leave 0.235 g (84%) of **2** as a colorless powder whose characterization data were identical to that of the crystals obtained above. mp: 220 °C (dec) gray-brown solid. Anal. Calcd (obsd): C, 24.03 (23.88); H, 2.59 (2.94); N, 10.01 (10.27). IR (KBr, ν_{CO} , cm^{-1}): 2034, 1922, 1899. ^1H NMR (CD_3CN , 293 K): δ_{H} [twist-boat, 90% of signal (integrations relative to this species), see Figure 4 for labeling] 7.66 (s, br, 1H, tim- H_a), 7.58 (s, br, 1H, tim- H_a), 7.50 (s, br, 1H, tim- H_b), 7.46 (s, br, 1H, tim- H_b), 3.89 (AB multiplet, $J_{\text{AB}} = 14.9$ Hz, $\Delta\nu = 1.0$ Hz, 2H, CH_2), 3.83 (br, s, 6H, NCH_3), 2.27 (br, s, 3H, CCH_3); [boat-chair, 10% of signal (integrations relative to this species)] 7.48 (d, $J = 1.7$ Hz, 2H, tim- H_a), 7.25 (d, $J = 1.7$ Hz, 2H, tim- H_b), 4.30 (AB multiplet, $J_{\text{AB}} = 14.8$ Hz, $\Delta\nu = 40.2$ Hz, 2H, CH_2), 3.72 (br, s, 6H, NCH_3), 2.14 (br, s, 3H, CCH_3). ^{13}C NMR (CD_3CN , 233 K): δ_{C} 194.0, 194.7, 142.32, 142.27, 136.2, 134.3, 127.5, 127.1, 123.6, 44.5, 35.62, 35.60, 4.3. ESI(+) MS: 552 (100) [$\text{M} - \text{Br} + \text{CH}_3\text{CN}$], 511 (40) [$\text{M} - \text{Br}$], 411 (14) [$\text{Re}(\text{CO})_3(\text{CH}_3\text{CN})_3(\text{H}_2\text{O})^+$], 270 (27) [$\text{Re}(\text{CO})_3^+$]. HRMS Calcd (obsd) for $\text{C}_{14}\text{H}_{15}\text{N}_5\text{O}_3\text{ReS}_2$ [M^+]: 550.0146 (550.0139). Single crystals suitable for X-ray diffraction were grown by layering a concentrated acetonitrile solution of **2** with Et_2O and allowing solvents to slowly diffuse over 2 days.

X-ray Crystallography. X-ray intensity data from a colorless hexagonal rod of $\text{Re}(\text{CO})_3\text{Br}[\text{CH}_2(\text{S-tim})_2]$ (**1**) were measured at 150(1) K on a Bruker SMART APEX CCD-based diffractometer, while those for a colorless plate of $\{\text{Re}(\text{CO})_3(\text{CH}_3\text{CN})[\text{CH}_2(\text{S-tim})_2]\}(\text{PF}_6)$ (**2**) were measured at 100(2) K on a Bruker SMART diffractometer equipped with an APEX2 CCD-based detector for the data collection of **2**. Both experiments used monochromatic Mo $\text{K}\alpha$ radiation, $\lambda = 0.71073$ Å.⁸ Raw data frame integration and L_p corrections were performed with SAINT+.⁸ Final unit cell parameters were determined by least-squares refinement of 6976 reflections from the data set of **1** and of the strongest 7600 reflections from the data set of **2**, each with $I > 5\sigma(I)$. The analysis of the data showed negligible crystal decay during collection. The data were corrected for absorption effects with SADABS.⁸ Direct

(6) Schmidt, S. P.; Trogler, W. C.; Basolo, F. *Inorg. Synth.* **1990**, *28*, 160.

(7) Hevia, E.; Perez, J.; Riera, V.; Miguel, D.; Kassel, S. Rheingold, A. *Inorg. Chem.* **2002**, *41*, 4673.

(8) SMART, version 5.625; SAINT+, version 6.22; SADABS, version 2.05; Bruker Analytical X-ray Systems, Inc.: Madison, WI, 2001.

Table 1. Crystallographic Data for $\text{Re}(\text{CO})_3\text{Br}[\text{CH}_2(\text{S-tim})_2]$ (**1**) and $\{\text{Re}(\text{CO})_3(\text{CH}_3\text{CN})[\text{CH}_2(\text{S-tim})_2]\}(\text{PF}_6)$ (**2**)

	$\text{Re}(\text{CO})_3\text{Br}[\text{CH}_2(\text{S-tim})_2]$	$\{\text{Re}(\text{CO})_3(\text{CH}_3\text{CN})[\text{CH}_2(\text{S-tim})_2]\}(\text{PF}_6)$
formula	$\text{C}_{12}\text{H}_{12}\text{BrN}_4\text{O}_3\text{ReS}_2$	$\text{C}_{14}\text{H}_{15}\text{F}_6\text{N}_5\text{O}_3\text{PReS}_2$
fw	590.49	696.60
cryst syst	hexagonal	orthorhombic
space group	P_622	$Pbca$
<i>a</i>	8.6926(3) Å	13.635(2) Å
<i>b</i>	8.6926(3) Å	13.746(2) Å
<i>c</i>	40.452(2) Å	23.788(4) Å
α	90°	90°
β	90°	90°
γ	120°	90°
<i>V</i>	2647.11(19) Å ³	4458.6(12) Å ³
<i>Z</i>	6	8
<i>T</i> (K)	150(1)	100(2)
ρ_{calcd}	2.222 Mg m ⁻³	2.076 Mg m ⁻³
$\mu(\text{Mo K}\alpha)$	9.403 mm ⁻¹	5.786 mm ⁻¹
R1 [<i>I</i> > 2 σ (<i>I</i>)] ^a (all data)	0.0327 (0.0328)	0.0184 (0.0225)
wR2 ^b (all data)	0.0777 (0.0777)	0.0440 (0.0453)

methods structure solution, difference Fourier calculations, and full-matrix least-squares refinement against F^2 were performed with SHELXTL.⁹

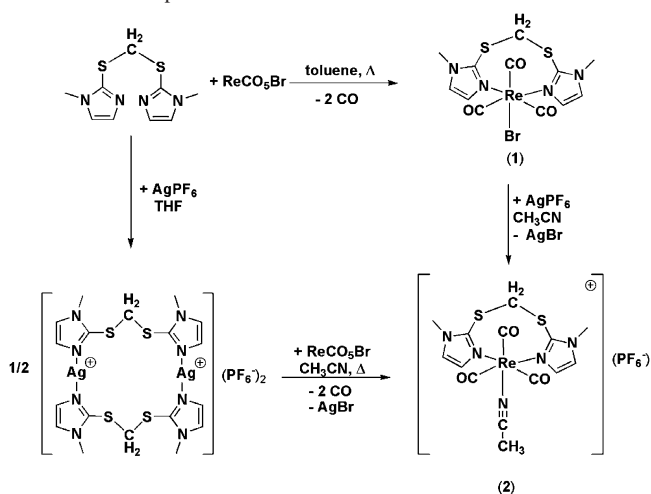
$\text{Re}(\text{CO})_3\text{Br}[\text{CH}_2(\text{S-tim})_2]$ (**1**) crystallizes in the hexagonal system. Systematic absences in the intensity data indicated a space group from either of the enantiomorphous pairs P_6/P_6 or P_622/P_622 . The space group P_622 was eventually confirmed by the successful solution and refinement of the data and supported by the final absolute structure (Flack) parameter of 0.04(3). The asymmetric unit contains half a molecule located on a 2-fold rotational axis. Re1 and C1 are on the 2-fold. The molecule is disordered about the 2-fold axis such that Br1 and the carbonyl group C22–O22 are interchanged. Occupancies for the Br1 and C22–O22 groups were initially refined and yielded values near the expected 0.5. Subsequently, these occupancies were fixed at 0.5 for the final refinement cycles. Refinement in P_6 with the 2-fold axis removed resulted in the same Br/CO disorder with one complete molecule per asymmetric unit. Since the disorder is still observed in the lower space group P_6 , it is not imposed by the 2-fold axes present in the higher space group P_622 , and therefore, P_622 was retained as the better space group choice. Careful examination of the intensity data showed no evidence of a larger unit cell which might resolve the disorder. All non-hydrogen atoms were refined with anisotropic displacement parameters except C22 and O22 (isotropic). Hydrogen atoms were placed in geometrically idealized positions and included as riding atoms.

$\{\text{Re}(\text{CO})_3(\text{CH}_3\text{CN})[\text{CH}_2(\text{S-tim})_2]\}(\text{PF}_6)$ (**2**) crystallizes in the orthorhombic system. Space group $Pbca$ was unequivocally assigned from systematic absences. The molecule is positioned in a general symmetry position and was refined in anisotropic approximation for all non-hydrogen atoms. The positions of the hydrogen atoms were determined from a series of difference Fourier syntheses and refined with isotropic approximation.

Results and Discussion

Synthesis. $\text{Re}(\text{CO})_3\text{Br}[\text{CH}_2(\text{S-tim})_2]$ (**1**) and $\{\text{Re}(\text{CO})_3(\text{CH}_3\text{CN})[\text{CH}_2(\text{S-tim})_2]\}(\text{PF}_6)$ (**2**) were prepared in high

(9) Sheldrick, G. M. *SHELXTL*, version 6.1; Bruker Analytical X-ray Systems, Inc.: Madison, WI, 2000.

Scheme 1. Preparation of Rhenium Derivatives**Table 2.** IR Spectroscopic Data for *fac*- $\text{Re}(\text{CO})_3(\text{ligand})$ *N,N*-Chelate Complexes

	ν_{CO} (KBr, cm ⁻¹)	ref
$\text{Re}(\text{CO})_3\text{Br}[\text{CH}_2(\text{S-tim})_2]$ (1)	2016, 1902, 1871	this work
$\text{Re}(\text{CO})_3\text{Br}(\text{bpy})$	2019, 1919, 1895	10a
$\text{Re}(\text{CO})_3\text{Br}(4,4'\text{-Me}_2\text{bpy})$	2019, 1889	10b
$\text{Re}(\text{CO})_3\text{Br}(1,4\text{-diazabutadiene})$	2025, 1925, 1910	10c
$\text{Re}(\text{CO})_3\text{Br}[\text{CH}_2(\text{pz})_2]$	2029, 1925, 1876	11
$\{\text{Re}(\text{CO})_3(\text{CH}_3\text{CN})[\text{CH}_2(\text{S-tim})_2]\}(\text{PF}_6)$ (2)	2034, 1922, 1899	this work
$[\text{Re}(\text{CO})_3(\text{CH}_3\text{CN})(\text{bpy})][\text{B}(3,5\text{-}(\text{CF}_3)_2\text{C}_6\text{H}_3)_4]$	2044, 1943	7

yields (>80%) according to Scheme 1. Compound **2** (prepared by two different routes) was originally synthesized with the intention of comparing its spectroscopic and electrochemical properties with its charge-neutral counterpart and was later found to be critical for understanding the complex solution behavior of **1**. For this purpose, the silver complex in the bottom left of Scheme 1, which has been described previously,⁵ was found to be a convenient reagent for a one-step high yielding (94%) synthesis of **2** from ReCO_5Br . Both **1** and **2** are air- and light-stable colorless solids that are soluble in DMSO, DMF, and acetonitrile, slightly soluble in acetone, THF, or CH_2Cl_2 , and insoluble in Et_2O or hydrocarbon solvents.

IR Spectra. The solid-state IR spectra of **1** and **2** each showed three CO stretching bands expected for *fac*-rhenium complexes with local C_s symmetry.^{10,11} A summary of the CO stretching frequencies for derivatives with $\text{Re}(\text{CO})_3(\text{Br}$ or $\text{CH}_3\text{CN})(N,N\text{-chelate})$ cores is given in Table 2. As expected, the electron-poor cationic derivative **2** is less capable of participating in back-bonding interactions and, thus, has higher carbonyl stretching frequencies than its charge-neutral counterpart **1**. This is also observed when the

(10) (a) Stor, G. J.; Hartl, F.; van Outersterp, J. W. M.; Stufkens, D. J. *Organometallics* **1995**, *14*, 1115. (b) Taplosky, G.; Duesing, R.; Meyer, T. J. *Inorg. Chem.* **1990**, *29*, 2285. (c) Staal, L. H.; Oskam, A.; Vrieze, K. J. *Organomet. Chem.* **1979**, *170*, 235.

(11) Reger, D. L.; Brown, K. J.; Gardinier, J. R.; Smith, M. D. J. *Organomet. Chem.* **2005**, *690*, 1889.

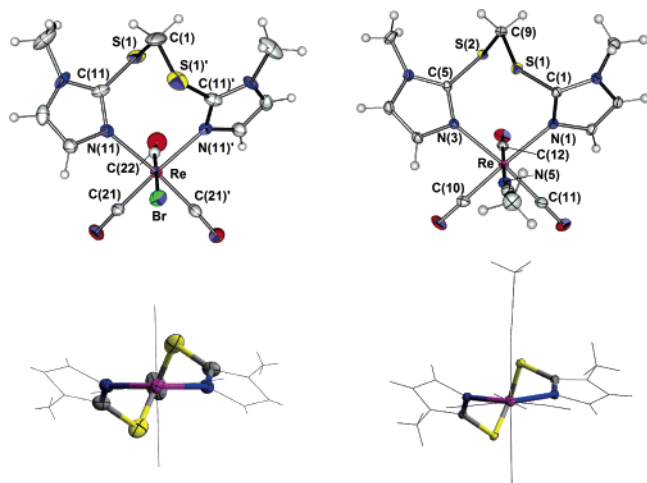


Figure 1. (left) Structure of one disordered component of $\text{Re}(\text{CO})_3\text{Br}[\text{CH}_2(\text{S-tim})_2]$ (**1**). Selected bond distances (Å) and angles (deg): $\text{Re}(1)-\text{C}(21) = 1.902(8)$, $\text{Re}(1)-\text{C}(22) = 1.92(2)$, $\text{Re}(1)-\text{N}(11) = 2.210(7)$, $\text{Re}(1)-\text{Br}(1) = 2.577(3)$, $\text{C}(21)-\text{O}(21) = 1.153(10)$, $\text{C}(22)-\text{O}(22) = 1.17(3)$; $\text{C}(21)-\text{Re}(1)-\text{Br}(1) = 90.1(3)$, $\text{C}(21)'\text{-Re}(1)-\text{Br}(1) = 94.7(3)$, $\text{C}(21)'\text{-Re}(1)-\text{C}(21) = 86.6(5)$, $\text{C}(21)'\text{-Re}(1)-\text{C}(22) = 91.8(6)$, $\text{C}(21)'\text{-Re}(1)-\text{C}(22) = 86.3(6)$, $\text{C}(22)-\text{Re}(1)-\text{C}(22)' = 177.4(11)$, $\text{C}(21)'\text{-Re}(1)-\text{N}(11) = 174.5(3)$, $\text{C}(22)'\text{-Re}(1)-\text{Br}(1) = 177.9(6)$. (right) Structure of $\{\text{Re}(\text{CO})_3(\text{CH}_3\text{CN})[\text{CH}_2(\text{S-tim})_2]\}(\text{PF}_6)$ (**2**). Selected bond distances (Å) and angles (deg): $\text{Re}(1)-\text{C}(10) = 1.907(2)$, $\text{Re}(1)-\text{C}(11) = 1.9157(19)$, $\text{Re}(1)-\text{C}(12) = 1.9172(19)$, $\text{Re}(1)-\text{N}(5) = 2.1404(16)$, $\text{Re}(1)-\text{N}(1) = 2.2119(14)$, $\text{Re}(1)-\text{N}(3) = 2.2233(14)$, $\text{C}(10)-\text{O}(10) = 1.158(2)$, $\text{C}(11)-\text{O}(11) = 1.148(2)$, $\text{C}(12)-\text{O}(12) = 1.150(2)$; $\text{C}(10)-\text{Re}(1)-\text{C}(11) = 88.43(8)$, $\text{C}(10)-\text{Re}(1)-\text{C}(12) = 88.19(8)$, $\text{C}(11)-\text{Re}(1)-\text{C}(12) = 88.77(8)$, $\text{C}(10)-\text{Re}(1)-\text{N}(5) = 94.91(7)$, $\text{C}(11)-\text{Re}(1)-\text{N}(5) = 94.49(7)$, $\text{C}(12)-\text{Re}(1)-\text{N}(5) = 175.56(7)$, $\text{C}(10)-\text{Re}(1)-\text{N}(1) = 174.53(7)$, $\text{C}(11)-\text{Re}(1)-\text{N}(1) = 86.13(7)$, $\text{C}(12)-\text{Re}(1)-\text{N}(1) = 92.23(7)$, $\text{N}(1)-\text{Re}(1)-\text{N}(5) = 84.98(6)$, $\text{C}(10)-\text{Re}(1)-\text{N}(3) = 89.62(7)$, $\text{C}(11)-\text{Re}(1)-\text{N}(3) = 176.57(7)$, $\text{C}(12)-\text{Re}(1)-\text{N}(3) = 93.99(6)$, $\text{N}(3)-\text{Re}(1)-\text{N}(5) = 82.87(6)$, $\text{N}(1)-\text{Re}(1)-\text{N}(3) = 95.79(5)$. The views at the bottom emphasize the twist-boat conformation of the eight-member chelate ring.

carbonyl stretching frequencies of $[\text{Re}(\text{CO})_3(\text{CH}_3\text{CN})(\text{bpy})]\text{-}(\text{B}[3,5\text{-}(\text{CF}_3)_2\text{C}_6\text{H}_3]_4)$ were compared with the charge-neutral halo-derivatives $\text{Re}(\text{CO})_3(\text{Cl}, \text{Br}, \text{or I})(\text{bpy})$.^{10,12} Also, by comparison of the CO stretching frequencies of **1** with those of the ReCO_3Br complexes of other N,N-chelating ligands (for samples prepared as KBr pellets), the electron-donating ability of $\text{CH}_2(\text{S-tim})_2$ ($\nu_{\text{CO}} = 2016, 1902, 1871 \text{ cm}^{-1}$) was found to be better than that of the dipyridyls (only two of the expected three bands are observed in many of the dipyridyl cases because of a fortuitous overlap of the lower energy stretches; the two observed bands typically occur near $\nu_{\text{CO}} = 2019, 1900 \text{ cm}^{-1}$) which are, in turn, better donors than the diazabutadienes ($\nu_{\text{CO}} = 2025, 1925, 1910 \text{ cm}^{-1}$), followed by the bis(pyrazolyl)methanes ($\nu_{\text{CO}} = \text{ca. } 2030, 1920, 1880 \text{ cm}^{-1}$).

Solid-State Structures. The structures of both $\text{Re}(\text{CO})_3\text{Br}[\text{CH}_2(\text{S-tim})_2]$ (**1**) and $\{\text{Re}(\text{CO})_3(\text{CH}_3\text{CN})[\text{CH}_2(\text{S-tim})_2]\}(\text{PF}_6)$ (**2**) are given in Figure 1. In each, the $\text{ReN}_2\text{C}_2\text{S}_2\text{C}$ eight-member chelate ring has a twist-boat geometry, as emphasized in the bottom of Figure 1. While the structure of **2** is well-behaved, that of $\text{Re}(\text{CO})_3\text{Br}[\text{CH}_2(\text{S-tim})_2]$ (**1**) is afflicted with a 50:50 disorder of the axial Br and CO groups that produces a pseudo-2-fold rotation axis along the $\text{C}(1)-\text{Re}$

vector that can be visualized in Figure S1 of the Supporting Information. The common metal–ligand bond distances in **1** and **2** are statistically identical and all are in agreement with values found in related systems.^{10–13} The similarity in the metal–ligand bond lengths in **1** and **2** signifies that the structural impact resulting from any difference in the back-bonding capabilities of the rhenium centers in each complex is, in fact, negligible. Also of potential structural significance is the intramolecular $\text{S}\cdots\text{S}$ distance, which may be important in determining the electrochemical activity of the ligands because of the possible formation of intramolecular disulfide linkages ($3.056(8) \text{ Å}$ in complex **1** and $3.069(2) \text{ Å}$ in **2**). Both distances are shorter than the corresponding distances (av 3.11 Å) in the silver complexes [with bridging $\text{CH}_2(\text{S-tim})_2$ ligands], which were, in turn, shorter than twice the van der Waals radii of sulfur.⁵

Solution Phase. Further characterization data shows that these two rhenium compounds, **1** and **2**, exhibit rich solution-phase chemistry. First, the ESI(+) mass spectrum of each compound in CH_3CN , which is thought to give one indication of the solution behavior of compounds,¹⁴ are nearly identical showing signals at $m/z = 552, 511$, and 270 (among others) that correspond to $\{\text{Re}(\text{CO})_3(\text{CH}_3\text{CN})[\text{CH}_2(\text{S-tim})_2]\}^+$, $\{\text{Re}(\text{CO})_3[\text{CH}_2(\text{S-tim})_2]\}^+$, and $[\text{Re}(\text{CO})_3]^+$, respectively. That is, the molecular ion is observed in **2** but not in **1**; the main fragmentation peak of **1** is from the unipositive complex, *sans* bromide. While the signal for the $\{\text{Re}(\text{CO})_3[\text{CH}_2(\text{S-tim})_2]\}^+$ ion is a result of the fragmentation process, both solution NMR and electrochemical studies indicate that the bromide dissociation to give $\{\text{Re}(\text{CO})_3(\text{CH}_3\text{CN})[\text{CH}_2(\text{S-tim})_2]\}^+$ occurs to a certain extent in CH_3CN under typical laboratory conditions (vide infra).

To facilitate the discussion of the NMR spectra of $\text{Re}(\text{CO})_3\text{Br}[\text{CH}_2(\text{S-tim})_2]$ (**1**) and $\{\text{Re}(\text{CO})_3(\text{CH}_3\text{CN})[\text{CH}_2(\text{S-tim})_2]\}(\text{PF}_6)$ (**2**), it will be useful to examine the expected NMR spectra of the possible isomers of these species in more detail. After possible interchanges of bromine (or acetonitrile in the case of **2**) and the axial carbonyl groups on rhenium, as well as what is known for other semirigid eight-member ring systems, such as *cis,cis*-1,4-cyclo-octadiene,¹⁵ its dibenzo analogue,¹⁶ or its heteroatomic dibenzo derivatives (**I–III**, respectively, Figure 2),¹⁷ are considered, it can be shown that there are seven possible conformers of the $\text{ReN}_2\text{C}_2\text{S}_2\text{C}$ ring in either **1** or **2** leading to a total of 10 isomers (including optical isomers), as shown for **1** in Figure 3. The relative stabilities of the various possible conformers were probed via the evaluation of the AM1 geometry-optimized structures

(12) Rossenaar, B. D.; Stufkens, D. J.; Vlcek, A., Jr. *Inorg. Chem.* **1996**, *35*, 2902.

(13) Reger, D. L.; Gardinier, J. R.; Pellechia, P. J.; Smith, M. D.; Brown, K. J. *Inorg. Chem.* **2003**, *42*, 7635.

(14) (a) Reger, D. L.; Wright, T. D.; Semeniuc, R. F.; Grattan, T. C.; Smith, M. D. *Inorg. Chem.* **2001**, *40*, 6212. (b) Reger, D. L.; Semeniuc, R. F.; Smith, M. D. *Eur. J. Inorg. Chem.* **2002**, 543. (c) Reger, D. L.; Semeniuc, R. F.; Smith, M. D. *Inorg. Chem. Commun.* **2002**, *5*, 278.

(15) Favini, G.; Zuccarello, F.; Bremi, G. *J. Mol. Struct.* **1969**, *3*, 385.

(16) Crossley, R.; Downing, A. P.; Nogradi, M.; Braga de Oliveira, A.; Ollis, W. D.; Sutherland, I. O. *J. Chem. Soc., Perkin I* **1973**, 205.

(17) Gellatly, R. P.; Ollis, W. D.; Sutherland, I. O. *J. Chem. Soc., Perkin I* **1976**, 913.

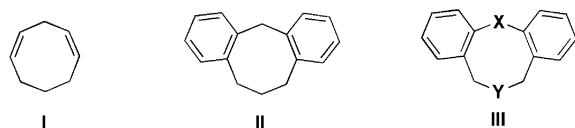


Figure 2. Semirigid organic-based eight-member ring systems. For **III**, X and Y can be carbon, any reasonable heteroatom, or heteroatom-containing groups such as S, SO₂, NH, etc.

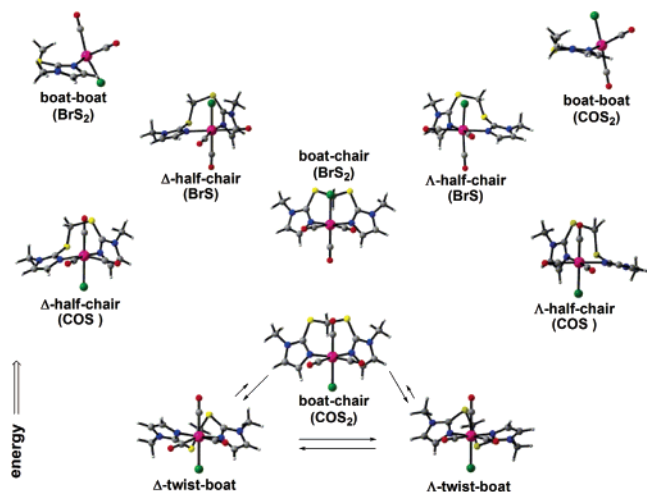


Figure 3. AM1 energy-minimized structures for seven different conformations (and 10 total isomers) of Re(CO)₃Br[CH₂(S-tim)₂] (**1**) calculated using SPARTAN molecular modeling software. The vertical displacement of each conformer (centered on the rhenium) from the lowest-energy twist-boat conformer approximates the relative energy.

calculated using the SPARTAN²⁴ molecular modeling program. While such models may be of limited value, certain qualitative features concerning factors responsible for the relative stabilities of the conformers become apparent, thereby allowing us to make more confident, yet still tentative, assignments for the two species responsible for the complicated NMR spectrum of **1** and **2** in acetone or CD₂-Cl₂ (vide infra). Gratifyingly, similar to the NMR spectral data, the calculations yield two (nearly isoergonic) low-energy conformers that can be distinguished from the remaining five conformers. These two low-energy conformers were the twist-boat (with C₁ symmetry) as found in the solid-state structure and the C_s-symmetric boat-chair with the CO oriented toward sulfurs. The remaining conformers could be differentiated in energy by consideration of the steric interactions between the sulfur atoms of the chelate ring and rhenium–bromide moiety: the more sulfur–bromine interactions, the higher in energy is the conformer. For instance,

- (18) Drago, R. S. *Physical Methods for Chemists*, 2nd ed.; Surfside Scientific Publishers: Gainseville FL, 1992; Chapter 7 and references therein.
- (19) Paudler, W. W. *Nuclear Magnetic Resonance*; Allyn and Bacon, Inc.: Boston, 1971; Chapter 6.
- (20) Kessler, H. *Angew. Chem., Intl. Ed. Engl.* **1970**, *9*, 219.
- (21) Gardinier, J. R. Unpublished observations.
- (22) Farona, M. F.; Kraus, K. F. *Inorg. Chem.* **1970**, *9*, 1700.
- (23) For example, see: (a) Schelter, E. J.; Bera, J. K.; Bacsa, J.; Galán-Mascarós, J. R.; Dunbar, K. R. *Inorg. Chem.* **2003**, *42*, 4256. (b) Helberg, L. E.; Orth, S. D.; Sabat, M.; Harman, W. D. *Inorg. Chem.* **1996**, *35*, 5584. (c) Helberg, L. E.; Barrera, J.; Sabat, M.; Harman, W. D. *Inorg. Chem.* **1995**, *34*, 2033. (d) Allison, J. D.; Fanwick, P. E.; Walton, R. A. *Organometallics* **1984**, *3*, 1515.
- (24) SPARTAN; Wavefunction, Inc.: Irvine, CA, 1997.

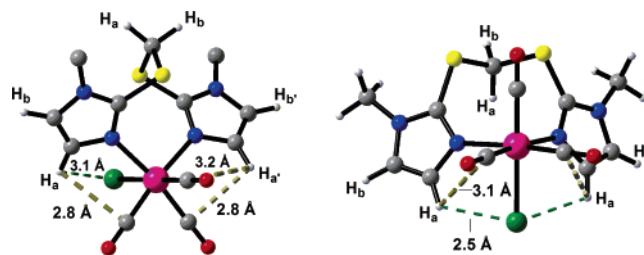


Figure 4. Labeling diagram used for NMR assignments. Important short intramolecular contact distances are also shown.

the C_s-symmetric boat-chair with bromine oriented toward the sulfurs is about 7 kcal/mol higher in energy than the other boat-chair. Also, because of considerable ring strain, the C_s-symmetric boat-boat conformers are about 25 kcal/mol higher in energy than the C_s-symmetric boat-chairs. Similar observations are obtained in the case where acetonitrile replaces bromine, as in **2**; however, the differences in energy between conformers were smaller presumably because of the lower steric demand of an acetonitrile versus a bromide. Thus, we interpret the complicated NMR spectra of **1** and **2** (in acetone or CD₂Cl₂) to result from a mixture of the twist-boat (with C₁ symmetry) and the C_s-symmetric boat-chair conformers with the CO oriented toward sulfurs.

Since the experimental NMR spectra can be satisfactorily interpreted to be the result of the presence of twist-boat and boat-chair (with CO oriented toward the sulfurs) conformers, the remainder of the discussion will be limited to these two cases. From Figure 4, it is expected that the NMR spectrum of the C₁-symmetric twist-boat conformer of **1** should consist of eight resonances: four thioimidazolyl hydrogen resonances (H_a, H_a', H_b, H_b'), two AB “doublet” resonances for the methylene hydrogens (H_a, H_b), and two *N*-methyl resonances. The expected spectrum of the C_s-symmetric boat-chair conformer should exhibit five resonances: two doublet resonances for thioimidazolyl hydrogens, two AB “doublet” methylene resonances, and a single *N*-methyl resonance. The corresponding spectra of the cation in **2** should have an additional resonance for the acetonitrile methyls.

The resonances for the thioimidazolyl and the methylene hydrogens of each conformer merit some further comment. First, the chemical shifts of the thioimidazolyl hydrogen resonances are anticipated to provide useful information regarding the local environment around rhenium. Changes in the environment around rhenium are expected to affect the chemical shifts of the hydrogen resonances in the ligand scaffold in a predictable way via dipole–dipole-type interactions, delineated by the Ramsey equation.¹⁸ That is, these interactions rapidly decrease with increasing distance (*E* is proportional to *r*⁻³) giving the relative order of impact: proximal thioimidazolyls > distal thioimidazolyls > *N*-methyls ≥ CH₂'s. Thus, the downfield-most thioimidazolyl hydrogen resonances that correspond to those hydrogens closest to the metal center are expected to be most affected by changes in the environment surrounding rhenium. In the C₁-symmetric twist-boat conformer of **1**, the proximal hydrogens are nearest in space to the equatorial carbonyls (Figure 4 left), but one hydrogen is oriented toward the axial

bromide and the other hydrogen toward the axial carbonyl, thereby differentiating these two hydrogens. As was seen in related systems,¹³ weak CH \cdots Br hydrogen bonding interactions tend to result in downfield shifts in hydrogen resonances. In the twist-boat conformer of **1**, the H \cdots Br distance is fairly long at 3.1 Å (from the X-ray structure), and because of the presumably weak nature of this CH \cdots Br interaction, only a small splitting of proximal thioimidazolyl hydrogen resonances is expected. In the boat-chair conformer with the axial CO oriented toward the sulfurs, the thioimidazolyl hydrogens proximal to rhenium are equivalent but are now nearest to the axial bromide on rhenium (rather than the equatorial CO ligands as in the twist-boat). In this low-energy conformer, the thioimidazolyl hydrogens are now only ca. 2.5 Å from the bromide (from the energy-minimized calculated structure); thus, a large downfield shift is expected for these resonances. Importantly, large chemical shift differences of proximal thioimidazolyl hydrogen resonances are expected in the spectrum of the boat-chair conformer (with CO oriented toward the sulfurs) of **1** compared to that of **2** because of the gross changes in the axial ligating sites in **1** versus **2**, where the chemical shifts may be modified by weak CH \cdots Br and CH \cdots π (CH₃CN) interactions, respectively. By analogy, the chemical shifts of the proximal thioimidazolyl hydrogen resonances for the twist-boat conformers of **1** and **2** should have greater similarity than the corresponding resonances of the boat-chair conformers of these compounds because of the nearly identical CH \cdots π (CO_{equatorial}) interactions: the differences in the spectra would be caused by long-range CH \cdots Br and CH \cdots π (CH₃CN) interactions. As indicated by the solid-state structural studies, any differences as a result of the different back-bonding capabilities of the metal center or because of the trans effect modulating the strength of otherwise similar (thioimidazolyl)-CH \cdots π (CO) interactions is expected to be minimal. Similarly, for the other possible (high-energy) boat-chair conformers of **1** and **2** with a carbonyl oriented between thioimidazolyl hydrogens, only minimal differences in the mean chemical shifts of thioimidazolyl resonances are expected.

The ¹H NMR spectra of **1** and **2** in various solvents is more complicated than expected from the solid-state structures because of (i) the equilibrium ionization of Re(CO)₃Br[CH₂(*S*-tim)₂] to give {Re(CO)₃(CH₃CN)[CH₂(*S*-tim)₂]⁺(Br⁻), (ii) the presence of equilibrium mixtures of interconvertible conformers of the complexes that comes from the conformational flexibility of the eight-member ReN₂C₂S₂C chelate ring, or (iii) both. Thus, the ¹H NMR spectra of **2** in CH₃CN contains 15 resonances, expected for a mixture of twist-boat and boat-chair isomers. However, the NMR spectrum of an analytically pure sample of **1** in CH₃CN has 28 resonances: 15 of these resonances match the chemical shifts of those in **2**, while the remaining 13 resonances are for a mixture of twist-boat and boat-chair conformers of complex **1**. For **1** in acetone or CH₂Cl₂ (Supporting Information), the total number of resonances drops to thirteen, again, for a mixture of twist-boat and boat chair isomers of the intact complex. Thus, the ionization of Re(CO)₃Br[CH₂(*S*-

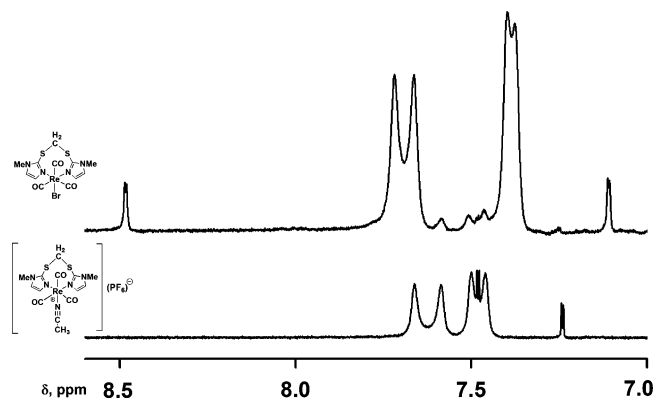


Figure 5. Downfield portion of the ¹H NMR spectrum of Re(CO)₃Br[CH₂(*S*-tim)₂] (top) and {Re(CO)₃(CH₃CN)[CH₂(*S*-tim)₂]}(PF₆) (bottom) in CD₃CN at 293 K.

tim)₂] to give {Re(CO)₃(CH₃CN)[CH₂(*S*-tim)₂]⁺(Br⁻) occurs in acetonitrile (and more polar solvents such as DMF and DMSO) but does not appear to occur to any appreciable extent in less polar (or possibly less nucleophilic) solvents. This is shown in Figure 5, which provides the downfield portion of the NMR spectrum (for thioimidazolyl resonances) of **1** (top) and of **2** (bottom) in acetonitrile at 293 K. The spectrum of analytically pure **1** in CD₃CN (top of Figure 5) clearly contains resonances in the baseline at ca. $\delta = 7.6$, 7.5, and 7.25 ppm that are for the {Re(CO)₃(CH₃CN)[CH₂(*S*-tim)₂]⁺ cation (bottom Figure 5, the nature of these resonances will be described later). An NMR-scale reaction between **2** and NBu₄Br in CD₃CN gave a spectrum identical to that of an independently prepared mixture of **1** and NBu₄PF₆ in the same solvent, verifying the equilibrium. The apparent equilibrium constant for the ionization of pure **1** in CH₃CN at 293 K is 4.3×10^{-3} (assuming the density of the CH₃CN in the solution is close to that for pure CH₃CN at 293 K so that the equilibrium concentration of CH₃CN is 19.1 M).

The broad nature of the resonances for the twist-boat conformer and the presence of small amounts of the boat-chair conformer compelled us to acquire variable-temperature NMR spectra to obtain thermodynamic and kinetic parameters associated with the variety of processes that occur in solutions of each compound. Some results of these studies are provided in Figure 6 and in Figures S4 and S5 in the Supporting Information. At 263 K and lower temperatures, the NMR spectra of **1** and **2** consist of sharp resonances indicative of slow exchange on the NMR time scale. Especially noteworthy in this temperature regime are the resonances for the thioimidazolyl hydrogens and those for the methylene moiety. First, the similarity in the mean chemical shifts of thioimidazolyl hydrogen resonances in the twist-boat conformers of **1** and **2** is indicative of the minimal structural impact of different metal–carbonyl back-bonding in each complex. By analogy, the very large difference in the chemical shifts of the proximal thioimidazolyl hydrogen resonances in the boat-chair conformers of **1** and **2** provides support that this conformer is indeed that with the carbonyl oriented toward sulfurs as from the earlier discussion. Also, on first inspection, the methylene resonance of the twist-

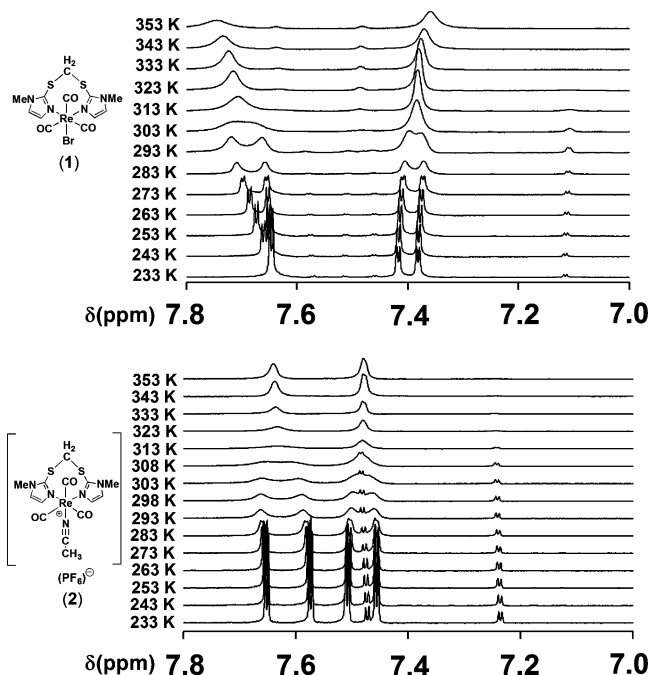


Figure 6. Identical portions of the ^1H NMR spectrum of $\text{Re}(\text{CO})_3\text{Br}[\text{CH}_2(\text{S-tim})_2]$ (**1**, top) and $\{\text{Re}(\text{CO})_3(\text{CH}_3\text{CN})[\text{CH}_2(\text{S-tim})_2]\}(\text{PF}_6)$ (**2**, bottom) in CD_3CN at various temperatures revealing the dynamic behavior of the $\{\text{Re}(\text{CO})_3(\text{CH}_3\text{CN})[\text{CH}_2(\text{S-tim})_2]\}^+$ cation in both **1** and **2**. See Supporting Information for full spectra.

boat conformer of **2** at room temperature appears to be a singlet, but the variable-temperature studies confirm that this is actually an AB multiplet. The intensity of the outer lines of an AB spectrum, I , from theory can be calculated from $I = 1 - \frac{1}{2}J_{AB}/\{1/2[(\Delta\nu)^2 + J_{AB}^2]^{1/2}\}$,^{18,19} where J_{AB} is the geminal coupling constant and $\Delta\nu$ is the chemical shift difference between resonances. The chemical shift difference of the resonances is very small, on the order of 6 Hz for **1** and 1 Hz for **2**, and the signals for the outer lines of the AB multiplet patterns are of very low intensity, almost indiscernible in the baseline.

When solutions of either **1** or **2** are warmed to room temperature and above, the various resonances for the twist-boat conformer broaden and coalesce between 293 and 303 K for **1** and between 303 and 308 K for **2**. At higher temperatures, the resonances for the boat-chair conformer broaden into the baseline and are no longer observed above 323 K. These results are interpreted by consideration of the two independent processes that interconvert twist-boat isomers: a low-energy twist-boat to twist-boat conversion and a higher but energetically accessible twist-boat to boat-chair to twist-boat conversion, as shown in the bottom portion of Figure 3. It should be noted that, similar to that found in the organic ring systems described earlier, the symmetric boat-chair isomers are more conformationally rigid than the twist-boat conformers. An examination of the CPK models supports the plausibility of a dual-pathway dynamic process, as it is found that simple torsion about the sulfur–methylene carbon bonds is sufficient to interconvert between two mirror-image twist-boat conformations, whereas a ring-flipping, in addition to bond torsion, is necessary to obtain the boat-

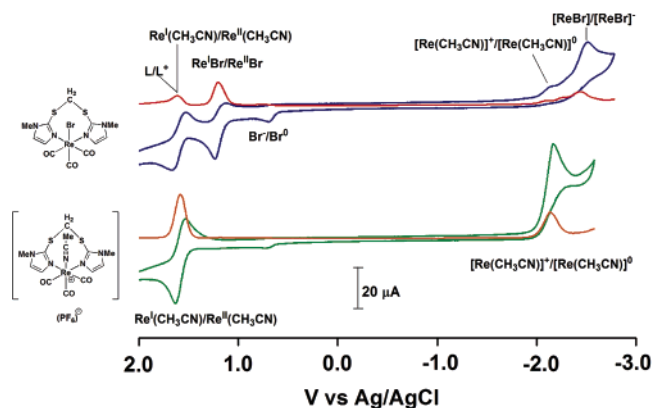


Figure 7. Cyclic and square-wave voltammograms of $\text{Re}(\text{CO})_3\text{Br}[\text{N},\text{N}-\text{CH}_2(\text{S-tim})_2]$ in CH_3CN (top) and $\{\text{Re}(\text{CO})_3(\text{CH}_3\text{CN})[\text{N},\text{N}-\text{CH}_2(\text{S-tim})_2]\}^+(\text{PF}_6)$ (bottom) in CH_3CN (NBu_4PF_6) at 50 mV/s.

chair conformer. From the relative integrations of resonances, it was found that the twist-boat is favored over the boat-chair by about 16:1 and 9:1 for **1** and **2**, respectively, at 293 K in all solvents tested (CD_2Cl_2 for **1**; acetone and CH_3CN for **1** and **2**). This equilibrium distribution corresponds to free-energy differences of about 1.7 and 1.2 kcal/mol between the two conformers of each respective compound, values close to those predicted by the molecular mechanics calculations. The measurement of K_{eq} from the integrations of thioimidazolyl resonances at temperatures between 283 and 233 K (where reliable integrations could be obtained) allowed for the determination of $\Delta H = -5.0$ kJ/mol, $\Delta S = -6.6$ J/Kmol and $\Delta H = -2.9$ kJ/mol, $\Delta S = -8.0$ J/Kmol for the boat-chair \rightleftharpoons twist-boat equilibrium for **1** and **2**, respectively, from the straight-line plots of $\ln K$ versus $(1/T)$. The coalescence temperature (T_c) of the thioimidazolyl resonances for the twist-boat to twist-boat conversion for each **1** and **2** was used to estimate statistically identical activation barriers of $E_a = 4.57T_c[10.32 + \log(\sqrt{2T_c}/\pi\Delta\nu)] = 18.6 \pm 0.3$ kcal/mol for **1** and $E_a = 19.2 \pm 0.3$ kcal/mol for **2** (where $\Delta\nu$ is the chemical shift difference of the resonances in absence of exchange).²⁰ Similar calculations were used provide crude estimations of $E_a = 22.0 \pm 0.5$ kcal/mol for the activation energy of the boat-chair to twist-boat conversion in **1** and **2**. In these latter calculations, a greater degree of uncertainty is introduced because of the disparity in relative populations of the boat-chair and twist-boat conformers, since a coalescence temperature is not easily obtained. Thus, the temperatures just before the resonances for the boat-chair conformers broaden into the baseline (323 K for **1** and 333 K for **2**) were used in the estimation. The calculated energies are of similar magnitude, but they are a little higher than observed for the ring-flipping mechanisms in cyclooctatetraene and in related eight-member organic ring systems.^{15–17}

Electrochemical Studies. The cyclic and square-wave voltammograms for compounds **1** and **2** are given in Figure 7. In support of the findings of the NMR spectroscopic studies, the electrochemical data are also indicative that $\text{Re}(\text{CO})_3\text{Br}[\text{CH}_2(\text{S-tim})_2]$ undergoes ionization in acetonitrile to give $\{\text{Re}(\text{CO})_3(\text{CH}_3\text{CN})[\text{CH}_2(\text{S-tim})_2]\}^+(\text{Br}^-)$. The ionization

of **1** in acetonitrile is most clearly evident from the small irreversible (anodic) oxidation wave at ca. +0.7 V versus Ag/AgCl (top of Figure 7) for the Br⁻/Br₂ couple which is nearly identical to the potential found for pure NBu₄Br in CH₃CN measured under the same conditions. Moreover, there are corresponding waves of similar (weak) intensity for the {Re(CO)₃(CH₃CN)[CH₂(*S*-tim)₂]}⁺ cation present in CH₃CN solutions of **1**. Thus, the voltammogram for **1** in acetonitrile consists of four oxidation waves, two overlapping waves at +1.58 and +1.53 V (best detected by square-wave voltammetry, by varying scan rates because of the significantly different diffusion rates, or by both), a wave at +1.17 V, and one at +0.7 V, in addition to two reduction waves at -2.17 and -2.52 V. For comparison, the voltammogram of **2** consists of one reversible oxidation wave at +1.58 V and one irreversible reduction wave at -2.17 V. Thus, in the voltammogram of **1**, only the three intense waves at +1.53, +1.17, and -2.52 V are from the redox processes involving the intact charge-neutral Re(CO)₃Br[CH₂(*S*-tim)₂] complex.

We can confidently assign the irreversible oxidation wave for **1** at +1.17 V to be from the Re^I/Re^{II} couple by a comparison of this potential with those found in other well-known tricarbonylrhenium(I) complexes of N,N-chelating ligands measured under similar conditions.^{10–13} For instance, in the series of compounds [ReBr(CO)₃(pz)₂CHC₅H₄Fe],¹¹ ReBr(CO)₃[CH₂(pz)₂],¹¹ ReBr(CO)₃[CMe₂(pz)₂],¹³ and ReBr(CO)₃[CH₂(3,5-Me₂pz)₂],²¹ the rhenium oxidation waves were found to be +1.40, +1.37, +1.35, and +1.29 V, respectively, versus Ag/AgCl measured under the same conditions as compound **1**. This order shows that changing substituents on the bis(pyrazolyl)methane ligand system has a small but significant impact on the Re^I/Re^{II} couple: the more electron rich the ligand the easier it is to oxidize rhenium and the lower the oxidation potential. Similar comparisons can be made to gauge the relative electron-donating abilities of closely related ligand systems. Thus, in support of the findings of the IR spectroscopic data for CO stretches, the electrochemical data for compound **1** with an oxidation potential of +1.17 V shows that the N,N-chelating CH₂(*S*-tim)₂ ligand is a better electron-donor than the dipyriddy [Re(CO)₃Br(bpy), *E*_{1/2} = +1.29 V versus Ag/AgCl] or any of the bis(pyrazolyl)methane ligands (*E*_{1/2} = +1.4 to +1.3 V). In the cationic derivative, {Re(CO)₃(CH₃CN)[CH₂(*S*-tim)₂]}(PF₆), **2**, the corresponding wave is shifted to more positive potentials (+1.58 V), as expected from Coulombic arguments. Interestingly, the metal-centered oxidation is now fully reversible in **2**, whereas it is irreversible in **1**.

The second most intense oxidation wave for intact Re(CO)₃Br[CH₂(*S*-tim)₂] (**1**) in CH₃CN at +1.53 V is assigned to a one-electron ligand oxidation. This assignment is made by comparison with the potentials found in the free ligand (+1.2 V) and its silver complexes (+1.5 V).^{3,5} Complexation to the electron-withdrawing bromotricarbonylrhenium moiety makes the ligand oxidation more difficult by 0.3 V, similar to the effect caused by complexation to silver(I) cations. In the case of **2**, the expected increased difficulty for the formation of a tricationic species (after the first metal

oxidation of monocationic **2**⁺ to give dicationic **2**²⁺, followed by ligand oxidation to give **2**³⁺) likely renders the first ligand oxidation so unfavorable as to be outside of the solvent potential window.

The nature of the reduction waves below -2.0 V versus Ag/AgCl for **1** and **2** is ambiguous as to whether these are metal- or ligand-based, however, it is clear from the right side of Figure 7 that the reduction wave for the cation in **2** is present in the voltammogram of pure **1** dissolved in CH₃CN. In terms of potential assignment of these waves, we favor ligand-centered reductions because the related purely organic dicationic derivative {CH₂(μ-tim)₂CH₂}(PF₆)₂ showed an irreversible cathodic reduction wave at -1.2 V versus Ag/AgCl measured under similar conditions,³ therefore, a monocationic derivative is expected to have a reduction at more negative potential. As testament to the difficulty in this assignment, the voltammograms of Re(CO)₃(CH₃CN)₂Br²² gives an irreversible cathodic reduction wave at -2.41 V (in addition to a metal centered oxidation at +1.91 V versus Ag/AgCl in CH₃CN); however, as this potential approaches the solvent limit in our experiments, it is unclear as to whether this wave may be caused by reduction of the coordinated acetonitrile or reduction of the Re⁺ center. It should be noted that, if the Re³⁺, Re²⁺, Re¹⁺, and Re⁰ oxidation states for a given ligand system can be accessed, these redox couples (in nonaqueous environments) are usually each only separated by a approximately 1 V, much smaller than the potential separations in all of the above cases.²³ Further experiments are underway to determine the nature of the reduction waves near -2.0 V in these and related systems. Regardless of their exact nature, the expected trend of increasing ease of reduction with increasing positive charge on going from the monocationic {Re(CO)₃(CH₃CN)[CH₂(*S*-tim)₂]}⁺ (**2**, -2.18 V) to the charge-neutral starting complex Re(CO)₃Br[CH₂(*S*-tim)₂] (**1**, -2.52 V) is followed.

Conclusions

Two new tricarbonylrhenium complexes of the electroactive bis(1-methylthioimidazolyl)methane ligand Re(CO)₃Br[CH₂(*S*-tim)₂] (**1**) and {Re(CO)₃(CH₃CN)[CH₂(*S*-tim)₂]}(PF₆) (**2**) have been prepared. Although it was not possible to unequivocally establish the nature of all the redox processes in the rhenium complexes of this ligand, the multiple solid-state and solution characterization methods permitted further evaluation of the unique structural and electronic properties of the ligand, as well as the discovery of the unusual solution chemistry involving these rhenium complexes. From IR and electrochemical data, it is found that the bis(1-methylthioimidazolyl)methane ligand is more electron-rich than the dipyriddyls or the bis(pyrazolyl)methanes, two common classes of N,N-chelating ligands. The solution NMR data indicate both **1** and **2** are stereochemically nonrigid in solution, as a result of the flexible eight-member chelate ring. Importantly, both NMR and electrochemical data indicate that **1** undergoes spontaneous ionization to {Re(CO)₃(CH₃CN)[CH₂(*S*-tim)₂]}(Br) in acetonitrile, where the equilibrium constant for ionization at 293 K was found by NMR to be

4.3×10^{-3} . That this ionization does not occur in less polar solvents such as acetone implicates an associative mechanism for ionization, but further studies are needed to discern the mechanism of ionization. Studies are underway in our laboratory to determine the origin (whether electronic, steric, or both) and generality of the labilization of the axial ligands on these and other tricarbonylrhenium(I) N,N-chelate complexes.

Acknowledgment. We thank Bill Cotham and Mike Walla at the University of South Carolina for mass spectro-

metric measurements; J.R.G. also thanks Marquette University and the donors of the Petroleum Research Fund for support.

Supporting Information Available: Figures showing disorder in the solid-state structure of **1**, additional NMR spectra for **1** and **2**, and crystallographic information files (CIF). This material is available free of charge via the Internet at <http://pubs.acs.org>.

IC060765T